13. U. Prakht, Numerical Methods in the Mechanics of Fluids [Russian translation], Moscow (1973), pp. 174-182.
14. G. R. Shrager and V. A. Yakutenok, Inzh.-Fiz. Sb., Tomsk (1985), pp. 36-44.
15. G. I. Barenblatt, PMM, 16, No. 1, 67-78 (1952).

FLOW OF AN ANOMALOUS VISCOUS FLUID IN A CENTRIFUGAL JET NOZZLE

O. M. Sokovnin, I. V. Flegentov, and V. A. Polovnikov UDC 532.135

The motion of twisted flows of an anomalous viscous fluid subject to an exponential law has been studied numerically.

Centrifugal jet nozzles have found extensive application in chemical technology apparatus requiring uniform spraying densities (absorbers, wet dust collectors, hydraulic foam extinguishers). In this case, the spray medium is generally a form of an anomalous viscous fluid: solutions of surface-active materials, suspensions, etc.

Let us take a look at the flow of an anomalous viscous fluid subject to an exponential law in a centrifugal jet nozzle (Fig. 1). We will assume the regime of motion to be both steady-state and axisymmetric. We will separate the flow region into the following zones:

I) the peripheral flow, bounded by the conical surfaces of frame 1 and insert 2;

II) the central flow in the channel, with a threaded insert;

III) the zone in which the peripheral and central flows are mixed.

I. We will examine the motion of the fluid in a special orthogonal curvilinear coordinate system ℓ, φ, δ, with the ℓ axis coincident with the generatrix of the internal cone. We will assume in the solution that 1) the influence of mass forces on the flow of the fluid is negligibly small; 2) that the velocity in the direction of the δ axis is considerably smaller than the velocity in the direction of the ℓ axis. The system of differential equations of fluid motion with consideration of [1] will then assume the following form:

$$\rho V_l \frac{\partial V_l}{\partial l} - \frac{\rho V_\varphi^2 \sin\alpha}{\delta\cos\alpha - l\sin\alpha} = -\frac{\partial p}{\partial l} + K\frac{\partial}{\partial\delta}\left(E^{n-1}\frac{\partial V_l}{\partial\delta}\right) + \frac{KE^{n-1}\cos\alpha}{\delta\cos\alpha - l\sin\alpha}\frac{\partial V_l}{\partial\delta},$$

$$\rho V_l \frac{\partial V_\varphi}{\partial l} - \frac{\rho V_\varphi V_l \sin\alpha}{\delta\cos\alpha - l\sin\alpha} = K\frac{\partial}{\partial\delta}\left(E^{n-1}\frac{\partial V_\varphi}{\partial\delta}\right) + \frac{2KE^{n-1}\cos\alpha}{\delta\cos\alpha - l\sin\alpha}\frac{\partial V_\varphi}{\partial\delta}, \quad (1)$$

$$-\frac{\rho V_\varphi^2 \cos\alpha}{\delta\cos\alpha - l\sin\alpha} = -\frac{\partial p}{\partial\delta} + K\frac{\partial}{\partial l}\left(E^{n-1}\frac{\partial V_l}{\partial\delta}\right) - \frac{KE^{n-1}\sin\alpha}{\delta\cos\alpha - l\sin\alpha}\frac{\partial V_l}{\partial\delta}.$$

Here

$$E = \sqrt{\left(\frac{\partial V_l}{\partial\delta}\right)^2 + \left(\frac{\partial V_\varphi}{\partial\delta}\right)^2}.$$

The boundary conditions will be as follows:

$$V_l = V_\varphi = 0 \quad \text{for} \quad \delta = 0; \quad \delta = \delta_0. \quad (2)$$

Kirov Polytechnic Institute. Translated from Inzhenerno-Fizicheskii Zhurnal, Vol. 57, No. 6, pp. 900-906, December, 1989. Original article submitted June 29, 1988.

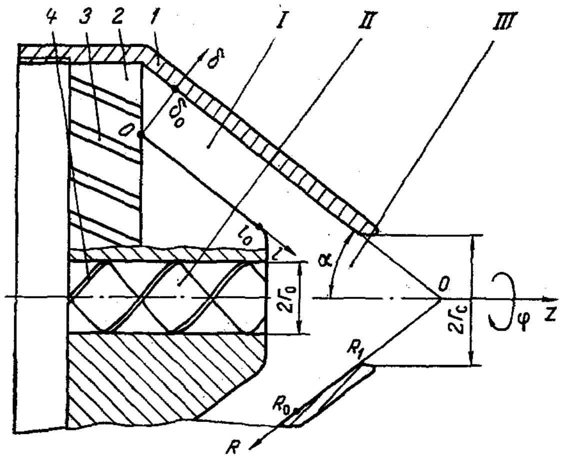

Fig. 1. Diagram of a centrifugal-jet nozzle, with the flow region divided into the following zones: I) peripheral flow zone; II) central flow zone; III) mixing zone. 1) frame; 2) insert; 3) peripheral-flow guide channels; 4) central channel with threaded insert.

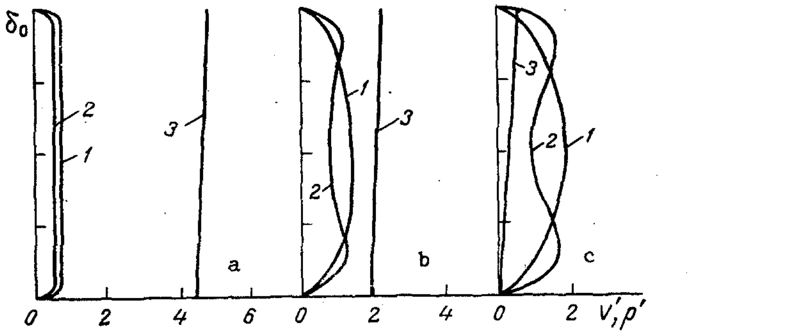

Fig. 2. Change in the velocities V_ℓ' (1), V_φ' (2), and in the pressure P' (3) along the length of the peripheral channel ($\tilde{Re}$ = 35, V_0 = 1 m/sec): a) $\ell = 0$; b) $\ell = 0.5\ell_0$; c) $\ell = \ell_0$.

We will specify the profiles of the velocity components in the inlet section of the channel in the following form: $V_{\ell 0} = \text{const}_1$, $V_{\varphi 0} = \text{const}_2$. Owing to the structural features of the nozzle (the angle of inclination for channels 3, twisting the peripheral flow, relative to the longitudinal axis, is no greater than 45°) with the twisting factor B in the case under consideration no greater than unity. We will solve the problem on a computer by an iteration method involving the utilization of a finite-difference scheme [2]. The grid dimension 10 × 9 (10 along the ℓ axis and 9 along the δ axis) with a constant interval along each of the axes. The channel walls in this case coincide with the boundary nodes of the grid along the δ axis, while the values of the velocities V_ℓ and V_φ at these nodes are set in accordance with boundary conditions (2). The iterations are curtailed as soon as the following conditions are satisfied, and namely:

$$\max_{i,j} |V^m_{i,j} - V^{m-1}_{i,j}| < 10^{-2}, \tag{3}$$

where m is the iteration number; $V_{i,j}$ is the value of the velocities at the (i, j) node of the grid.

The method that is usually used in such problems, i.e., the introduction of stream functions to eliminate pressure from system of equations (1), in the given case leads to significant mathematical difficulties due to the need to make provision for the variable viscosity of the fluid, dependent on the velocity of fluid motion through the channel. We will therefore determine the pressure directly from the third of the equations in system (1):

$$p = \int_0^\delta \left[\frac{V_\varphi^2 \cos\alpha}{\delta\cos\alpha - l\sin\alpha} + \frac{K}{\rho}\frac{\partial}{\partial l}\left(E^{n-1}\frac{\partial V_l}{\partial\delta}\right) - \frac{K}{\rho}\frac{E^{n-1}\sin\alpha}{\delta\cos\alpha - l\sin\alpha}\frac{\partial V_l}{\partial\delta}\right] d\delta + f(l), \tag{4}$$

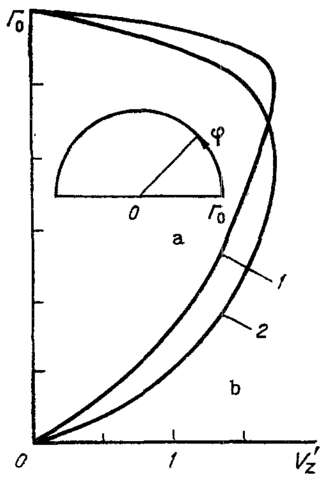

Fig. 3

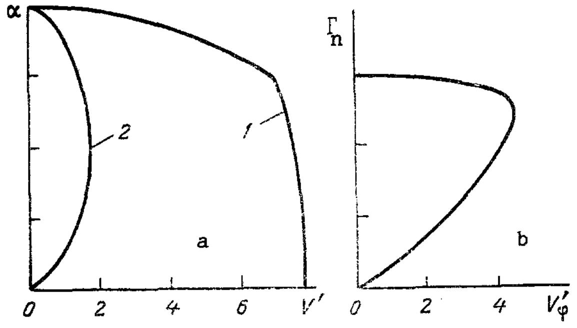

Fig. 4

Fig. 3. Profile of the velocity V_z' at the outlet from the central channel ($\tilde{R}e$ = 13.5, V_0 = 1 m/sec): a) lateral cross section of the central channel, separated by the threaded inserts; b) profile of V_z' for $\varphi = \pi/4$ (1), $\varphi = \pi/2$ (2).

Fig. 4. Velocity profiles in the outlet section of the nozzle ($\tilde{R}e$ = 252, V_0 = 1 m/sec): a) profiles V_R' (1), V_θ' (2); b) profile V_φ'.

which is solved by numerical integration.

Figure 2 shows the results from calculations with $\tilde{R}e$ = 35 and B = 0.83. Comparison of the derived profiles demonstrates that as motion proceeds through the channel the axial component of the velocity V_ℓ assumes a parabolic profile, whereas the circumferential velocity component V_φ forms a concave profile with its minimum at the central portion of the channel. No reverse flow arises in this case. The drop in pressure along the δ axis at various cross sections of the channel is insignificant, and the pressure profile is nearly rectangular, with some rise in pressure at the outside wall of the channel.

II. Let us introduce a system of helical coordinates z, φ, Γ [3], where the z axis coincides with the longitudinal axis of the nozzle. In our solution of this problem we will neglect the influence exerted by the mass forces and we will assume that 1) $V_\varphi \sim V_\Gamma \ll V_z$; 2) $\partial/\partial\Gamma \sim \partial/\partial\varphi \gg \partial/\partial z$; 3) the pressure drop across the channel is equal to the pressure drop across the peripheral channel. The system of equations of motion, in conjunction with the adopted assumptions, reduces to the following single equation:

$$KE^{n-1}\left(\frac{8\pi^2\Gamma}{4\pi^2\Gamma^2+S^2}+\frac{1}{\Gamma}\right)\left(\frac{\partial V_z}{\partial\Gamma}-\frac{4\pi^2\Gamma}{4\pi^2\Gamma^2+S^2}V_z\right)- -\frac{S}{\sqrt{4\pi^2\Gamma^2+S^2}}\frac{\partial p}{\partial z}+\frac{K}{\Gamma^2}\frac{\partial}{\partial\varphi}\left(E^{n-1}\frac{\partial V_z}{\partial\varphi}\right)+ +K\frac{\partial}{\partial\Gamma}\left[E^{n-1}\left(\frac{\partial V_z}{\partial\Gamma}-\frac{4\pi^2\Gamma}{4\pi^2\Gamma^2+S^2}V_z\right)\right]=0. \tag{5}$$

Here

$$E=\left[\left(\frac{1}{\Gamma}\frac{\partial V_z}{\partial\varphi}\right)^2+\left(\frac{\partial V_z}{\partial\Gamma}-\frac{4\pi^2\Gamma}{4\pi^2\Gamma^2+S^2}V_z\right)^2\right]^{1/2}.$$

The boundary conditions have the form

$$V_z=0 \text{ when } \Gamma=\Gamma_0,\quad \varphi=0,\quad \varphi=\pi. \tag{6}$$

We will solve (5) by the method which was used in the solution of system (1) in a 7 × 13 grid. The resulting profile of the velocity $V_z = V(\Gamma, \varphi)$ at the outlet from the channel for the case in which $\tilde{R}e = 13.5$ is shown in Fig. 3. The profile of the axial velocity V_z increases smoothly from the center of the channel (divided by the plane of the helical insert) to the periphery. The maximum is attained for the case in which $\Gamma = (0.7\text{-}0.8)\Gamma_0$, dependent on the change in the circumferential coordinate φ.

III. The mixing zone is a converging conical channel. To describe the motion of the fluid in this zone, we will make use of a spherical coordinate system R, φ, Θ, whose center is situated on the longitudinal axis of the nozzle at the point at which it intersects with the generatrix of the external cone (see Fig. 1). If we assume that all of the velocity components and their derivatives in this zone are of the same order of magnitude and if we neglect the mass forces, we derive the following system of equations:

$$\rho\left(V_R\frac{\partial V_R}{\partial R}+\frac{V_\Theta}{R}\frac{\partial V_R}{\partial\Theta}-\frac{V_\Theta^2+V_\varphi^2}{R}\right)=-\frac{\partial p}{\partial R}+\frac{4KE^{n-1}}{R}\frac{\partial V_R}{\partial R}+$$
$$+2K\frac{\partial}{\partial R}\left(E^{n-1}\frac{\partial V_R}{\partial R}\right)+\frac{KE^{n-1}\operatorname{ctg}\Theta}{R}\left(\frac{\partial V_\Theta}{\partial R}+\frac{1}{R}\frac{\partial V_R}{\partial\Theta}-\frac{V_\Theta}{R}\right)+$$
$$+\frac{K}{R}\frac{\partial}{\partial\Theta}\left[E^{n-1}\left(\frac{\partial V_\Theta}{\partial R}+\frac{1}{R}\frac{\partial V_R}{\partial\Theta}-\frac{V_\Theta}{R}\right)\right]-$$
$$-\frac{2KE^{n-1}}{R^2}\left(\frac{\partial V_\Theta}{\partial\Theta}+\operatorname{ctg}\Theta V_\Theta+2V_R\right),$$
$$\rho\left(V_R\frac{\partial V_\Theta}{\partial R}+\frac{V_\Theta}{R}\frac{\partial V_\Theta}{\partial\Theta}+\frac{V_RV_\Theta}{R}-\frac{V_\varphi^2\operatorname{ctg}\Theta}{R}\right)=-\frac{1}{R}\frac{\partial p}{\partial\Theta}+$$
$$+\frac{KE^{n-1}\operatorname{ctg}\Theta}{R^2}\left(\frac{\partial V_\Theta}{\partial\Theta}+V_R\right)+\frac{2K}{R^2}\frac{\partial}{\partial\Theta}\left[E^{n-1}\left(\frac{\partial V_\Theta}{\partial\Theta}+V_R\right)\right]+$$
$$+\frac{2KE^{n-1}}{R}\left(\frac{\partial V_\Theta}{\partial R}-\frac{V_\Theta}{R}+\frac{1}{R}\frac{\partial V_R}{\partial\Theta}\right)+K\frac{\partial}{\partial R}\left[E^{n-1}\left(\frac{\partial V_\Theta}{\partial R}-\right.\right.$$
$$\left.\left.-\frac{V_\Theta}{R}+\frac{1}{R}\frac{\partial V_R}{\partial\Theta}\right)\right]-\frac{2KE^{n-1}\operatorname{ctg}\Theta}{R^2}(V_R+\operatorname{ctg}\Theta V_\Theta),$$
$$\rho\left(V_R\frac{\partial V_\varphi}{\partial R}+\frac{V_\Theta}{R}\frac{\partial V_\varphi}{\partial\Theta}+\frac{V_RV_\varphi}{R}+\frac{V_\varphi V_\Theta\operatorname{ctg}\Theta}{R}\right)=$$
$$=\frac{3KE^{n-1}}{R}\left(\frac{\partial V_\varphi}{\partial R}-\frac{V_\varphi}{R}\right)+K\frac{\partial}{\partial R}\left[E^{n-1}\left(\frac{\partial V_\varphi}{\partial R}-\frac{V_\varphi}{R}\right)\right]+$$
$$+\frac{2KE^{n-1}\operatorname{ctg}\Theta}{R^2}\left(\frac{\partial V_\varphi}{\partial\Theta}-\operatorname{ctg}\Theta V_\varphi\right)+\frac{K}{R^2}\frac{\partial}{\partial\Theta}\left[E^{n-1}\left(\frac{\partial V_\varphi}{\partial\Theta}-\operatorname{ctg}\Theta V_\varphi\right)\right],$$
$$R\frac{\partial V_R}{\partial R}+\frac{\partial V_\Theta}{\partial\Theta}+2V_R+\operatorname{ctg}\Theta V_\Theta=0. \qquad (7)$$

Here

$$E=\left[2\left(\frac{\partial V_R}{\partial R}\right)^2+\frac{2}{R^2}\left(\frac{\partial V_\Theta}{\partial\Theta}+V_R\right)^2+\frac{2}{R^2}(V_R+\operatorname{ctg}\Theta V_\Theta)^2+\right.$$
$$\left.+\left(\frac{\partial V_\Theta}{\partial R}-\frac{V_\Theta}{R}+\frac{1}{R}\frac{\partial V_R}{\partial\Theta}\right)^2+\left(\frac{1}{R}\frac{\partial V_\varphi}{\partial\Theta}-\frac{\operatorname{ctg}\Theta}{R}V_\varphi\right)^2+\left(\frac{\partial V_\varphi}{\partial R}-\frac{V_\varphi}{R}\right)^2\right]^{1/2}.$$

In this case, the velocity components at the channel walls are equal to zero, i.e.,

$$V_R=V_\varphi=V_\Theta=0 \text{ when } \Theta=\pm\alpha. \qquad (8)$$

As the initial conditions for the velocity values at the inlet to the zone, we will use the calculation results obtained in the solutions for the previous zones, taking into consideration the transition of these solutions to spherical coordinates. System of equations (7) is also solved by an iteration method involving the use of finite-difference schemes, and we find the velocity V_Θ here from the fourth of the equations in system (7) by integration:

$$V_\Theta = \frac{1}{\sin\Theta}\int_0^\Theta \left(-R\frac{\partial V_R}{\partial R} - 2V_R\right)\sin\Theta d\Theta. \quad (9)$$

Integration of (9) is introduced numerically. In calculating the mixing zone we choose a uniform grid with dimensions of 8 × 9 (8 along the R axis and 9 along the Θ axis). The specifics of the problem relate to the exposure of the indeterminacies of the form 0/0 found in the equations of system (7) and in Eq. (9) for the case in which Θ = 0. Here we make use of the l'Hôpital rule and the physical features of the flow $V_\varphi = V_\Theta = 0$ for the case in which Θ = 0. Using the following dimensionless quantities, we will introduce the solution of system (1), (5), and (7):

$$p' = \frac{p}{\rho V_0^2}; \quad V_i' = \frac{V_i}{V_0}; \quad K' = K\frac{V_0^{n-2}}{\rho a_0^n}, \quad (10)$$

here a_0 is the characteristic linear dimension for each of the zones being studied: I) $a_0 = \delta_0$; II) $a_0 = \Gamma_0$; III) $a_0 = \Gamma_n$. Figure 4 shows the velocity profiles V_R, V_φ, and V_Θ in the outlet section of the nozzle for $\tilde{R}e$ = 252.

Analysis of these graphs shows that the profile of the axial velocity V_R is nearly parabolic, and that this is accompanied by a significant velocity gradient at the channel walls, where it increases from zero to its maximum value. The profile of the circumferential velocity V_Θ attains its maximum near the walls, and then diminishes linearly to zero at the channel axis. The magnitude of the velocity V_φ changes according to the laws of a parabola assuming zero values at the walls and in the center of the channel. The change in V_Θ in this case occurs more smoothly than for V_R and V_φ. We should take note of the fact that as a consequence of axial symmetry in the case of Θ situated in the interval [−α, 0], the velocities V_φ and V_Θ change sign. The geometric channel dimensions and the initial values for the velocities $V_{\ell 0}$, $V_{\varphi 0}$, and V_{z0} used in the calculations for the nozzle shown in Fig. 1 are presented below:

δ_0, mm	l_0, mm	Γ_0, mm	α, rad	R_0—R_1, mm	Γ_c, mm	V_{l0}, m/sec	$V_{\varphi 0}$, m/sec	V_{z0}, m/sec
1,6	9,0	1,2	0,693	3,5	1,5	0,71	0,59	1,53

Utilization of this calculation method is limited by the conditions under which laminar flow is achieved within the mixing zone. Stable convergence of iterations is observed in the solution of system (7), when $\tilde{R}e \le 360$. With a larger value for $\tilde{R}e$ in the mixing zone we have the onset of flow agitation. It should be noted that for the first two zones the stable solution is obtained for $\tilde{R}e \le 7800$ and Re ≤ 6200, respectively. The laminar nature of the flow is retained in such channels for a considerably longer period of time than in cylindrical tubes, a fact which was pointed out in [4].

The derived fields for the velocities and pressures in the motion of an anomalous viscous fluid in a centrifugal-jet nozzle can be used to calculate the spray flare angle and the drop dispersion [5, 6] in the design of mass-exchange apparatus. Moreover, the method for the solution can be used in calculating the flows of anomalous viscous fluids in conical and helical channels such as those most frequently used in the mass-exchange equipment of chemical technology.

NOTATION

E, second invariant of the strain rate tensor, sec^{-1}; ρ, fluid density, kg/m^3; p, hydrostatic pressure, Pa; K, rheologic constant, $Pa \cdot c^n$; n, flow index; $V_{\ell 0}$, $V_{\varphi 0}$, V_{z0}, initial values of the axial and circumferential velocities in the peripheral channel and the axial velocity in the helical channel, m/sec; $B = V_{\varphi 0}/V_{\ell 0}$, twisting factor; V_ℓ, V_φ, V_z, axial and circumferential velocity in peripheral channel and axial velocity in helical channel, m/sec; δ_0, width of gap between cones forming the peripheral channel, m; α, slope of cone generatrix to the longitudinal nozzle axis, rad; S, pitch of the helical line, m; Γ_0, radius of helical channel, m; ℓ_0, length of peripheral channel, m; R_0—R_1, length of mixing zone, m; Γ_n, radius of nozzle, m; V_R, V_φ, V_Θ, axial, circumferential, and radial components of the fluid velocity in the mixing zone, m/sec; $\tilde{R}e = V^{2-n}a_0^n\rho/K$, modified Reynolds number for a non-Newtonian fluid; V_0, unit velocity, m/sec; $f(\ell)$, arbitrary integration function determined by the pressure difference across the channel.

LITERATURE CITED

1. N. Kh. Zinnatullin and I. V. Flegentov, in: Abstracts of the Kirov KKhTI, No. 48, 140-144 (1972).
2. P. Rouch, Computational Hydrodynamics [Russian translation], Moscow (1980).
3. J. Happel and G. Brenner, Hydrodynamics with Small Reynolds Numbers [Russian translation], Moscow (1976).
4. L. G. Loitsyanskii, The Mechanics of Liquids and Gases [in Russian], Moscow (1973).
5. D. G. Pazhi and V. S. Galustov, The Fundamentals of Fluid Spray Engineering [in Russian], Moscow (1984).
6. Yu. I. Khavkin, Centrifugal Nozzles [in Russian], Leningrad (1976).

MOTION OF A RAREFIED GAS IN A PLANE CHANNEL IN THE PRESENCE OF CONDENSATION ON THE CHANNEL WALLS

F. M. Sharipov and T. V. Shchepetkina

UDC 533.6.011.8

We examine the flow of a rarefied gas through a broad range of Knudsen numbers under the action of small pressure and temperature differences in a plane short channel, with provision made for the processes of evaporation and condensation at the channel walls.

The processing of mass transfer, in which provision is made for evaporation and condensation on the walls, have been studied in numerous papers, such as, for example [1-5]. The transport of gas between plane infinite plates is the subject of [1], while [2, 3] deal with the motion of a gas in an infinite pore and a number of simplifying assumptions have been made here; in [4] we find a study of the flow in a finite channel, but the gas flow rate and its dependence on the length of the channel and the flow regime have not been dealt with, and in this particular case the boundary conditions are specified for the ends of the channel. In [5] we find a study of the kinetics involved in the mass transfer that occurs under the action of a small pressure difference in a plane finite pore, with consideration given to vaporization and condensation at the walls and at the bottom of the pore. The boundary conditions are specified directly at the inlet to the pore. In the present paper we investigate the heat and mass transfer that arises under the action of small pressure and temperature drops across a finite channel, with consideration given to the evaporation and condensation that occurs on the channel walls over a broad range of Knudsen numbers. Unlike the earlier-cited studies, the flow of gas is treated here not only within the channel, but also in the regions externally adjacent to the channel.

Let us take a look at a plane channel of length ℓ, of height a, and infinite in width, as shown in Fig. 1, connecting two vessels containing the identical gas. At a rather large distance from the channel, the gas within the vessels is maintained under equilibrium conditions at pressures P_1 and P_2 and temperatures T_1 and T_2, respectively. Here the distribution functions are in the form of absolute Maxwellians:

$$f_i = \frac{P_i}{kT_i}\left(\frac{m}{2\pi kT_i}\right)^{3/2}\exp\left(-\frac{mv^2}{2kT_i}\right),\ i = 1, 2.$$

The walls of each of the vessels exhibit temperatures of T_1 and T_2, respectively. It is assumed that all of the molecules reaching the walls of the vessels are diffusely reflected, and absorbed as they impinge on the channel walls. The walls, in this case, radiate the molecules with the following distribution function:

Sverdlovsk Engineering Pedagogical Institute. Translated from Inzhenerno-Fizicheskii Zhurnal, Vol. 57, No. 6, pp. 906-912, December, 1989. Original article submitted June 13, 1988.

